Chemosphere 257 (2020) 127277

Contents lists available at ScienceDirect

Chemosphere

journal homepage: www.elsevier.com/locate/chemosphere

Pb^{2+} and Cd^{2+} recovery from water using residual tea waste and SiO_2@TW nanocomposites

Seema Joshi [a], Navish Kataria [b], V.K. Garg [a, c, *], K. Kadirvelu [d]

[a] *Department of Environmental Science and Engineering, Guru Jambheshwar University of Science and Technology Hisar, 125001, India*
[b] *Department of Environmental Sciences, J. C. Bose University of Science and Technology, YMCA, Faridabad, 121006, Haryana, India*
[c] *Centre for Environmental Sciences and Technology, Central University of Punjab, Bathinda, 151001, Punjab, India*
[d] *DRDO-BU Center for Life Sciences, Bharathiar University Campus, Coimbatore 641046, Tamilnadu, India*

HIGHLIGHTS

- Silica nanoparticles (nps) were fabricated by modified stober-method and were loaded on tea waste.
- Adsorption capacity of SiO_2@TW nanocomposites (ncs) was found 153 mg/g (Pb^{2+}) and 222.2 mg/g (Cd^{2+}) greater than Tea Waste.
- SiO_2@TW ncs showed good reusability than tea waste adsorbent.

GRAPHICAL ABSTRACT

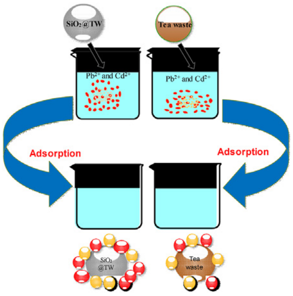

ARTICLE INFO

Article history:
Received 11 March 2020
Received in revised form
27 May 2020
Accepted 30 May 2020
Available online 3 June 2020

Handling Editor: Y Yeomin Yoon

Keywords:
Nanocomposites
Heavy metals
Kinetics
Stober method
Adsorption
Isotherms

ABSTRACT

This work reports the fabrication of SiO_2@TW nanocomposites and their application for Pb^{2+} and Cd^{2+} ions sequestration from simulated water. Residual tea waste has also been used for metal ions sequestration to compare the potential of SiO_2@TW nanocomposites. The SEM, TEM, BET, FTIR and EDX techniques were employed for the characterization of SiO_2@TW nanocomposites and residual tea waste. Particle sizes of SiO_2@TW nanocomposites was in the range of 6.8–12 nm. The experiments were carried out in batch mode to explore the effect of various operating parameters on the sequestration of Pb^{2+} and Cd^{2+} ions from water. The experimental data was subjected to various thermodynamic, kinetic and isothermic models. According to Langmuir model, the maximum adsorption efficiency of the SiO_2@TW nanocomposites was 153 mg/g for Pb^{2+} and 222 mg/g for Cd^{2+} but maximum adsorption efficiency of residual tea waste for Pb^{2+} was 125 mg/g and for Cd^{2+} was 142.9 mg/g. This study suggested that due to the presence of active sites SiO_2@TW nanocomposites has greater potential for metal sequestration than residual tea waste.

1. Introduction

Most of the heavy metals, such as chromium, lead, arsenic, cadmium etc., are detrimental and non-biodegradable. These are usually present in industrial wastewater and may contaminate surrounding environment including water bodies. These metals get

---

* Corresponding author. Centre for Environmental Sciences and Technology, Central University of Punjab, Bathinda, 151001, Punjab, India
E-mail address: vinodkgarg@yahoo.com (V.K. Garg).

https://doi.org/10.1016/j.chemosphere.2020.127277
0045-6535/

accumulated in natural surroundings and may intrude in the food chain. Thus it is important to sequester these metals from different environmental matrices. (Xiong et al., 2015). Lead is naturally present in the earth crust. Various anthropogenic activities viz, industrial operations, construction, ammunition, radiation and shielding etc. release lead in the environment. The higher level of inorganic lead results in lead poisoning which affects the reproductive and neurological systems and may prove fatal for living systems (Gautam et al., 2014; Zhu and Li. 2015). Cadmium does not exist naturally as a pure metal though it is available in the form of complex carbonates, oxides and sulphides (Gautam et al., 2014; Jain et al., 2013). It enters into environmental systems from cadmium-nickel batteries, mining, phosphatic fertilizers, sewage sludge, anti-corrosive metal coatings, plastic stabilizers, alloys, pigments, coal burning and neutron absorbers in nuclear reactors (Chowdhury and Yanful, 2013). Cadmium poisoning may cause psychological disorder, damage to immune system and nervous system, vomiting, deformities in skeleton, kidney failure, renal disorder etc. (Kataria and Garg, 2018b).

Presently numerous techniques are employed for the treatment of heavy metals' burdened wastewater. These methods include physical, chemical, biological, physico-chemical and bio-chemical treatments. Physico-chemical methods like coagulation, membrane separation, ion exchange and adsorption are valuable and effective in several ways. But there are some disadvantages too, which include higher cost of treatment, sludge generation etc. Some of these methods are not economically viable, if wastewater contains large quantities of heavy metals (Otero et al., 2009). Excessive amount of sludge production also cause pollution of soil, natural water systems etc. All the developed and developing nations are facing these challenges and are in search of new effective and economic alternatives for the removal of various pollutants from water.

The adsorption process is better, reliable and attractive alternative, especially if the adsorbent is cost effective (Bulgariu et al., 2013; Liu et al., 2018). In recent years nanoadsorbents are found to be promising and innovative alternative to traditional adsorbents due to their smaller size, higher surface area, higher regeneration efficiency, more reuse potential, higher thermal stability and magnetic nature (Garg and Kataria, 2016; Ahlawat et al., 2019). On the other side, traditional adsorbents derived from plants such as tea waste, orange peel waste, walnut waste, rice husk, saw dust etc are proved to be effective adsorbents for heavy metals' removal from wastewater further when nanomaterials were loaded on them their efficiency and adsorption properties are enhanced due to the formation of nanocomposites (Kataria and Garg, 2019; Chauhan et al., 2020).

Tea is one among the most used beverages which is extracted from the leaves of tea plant, *Camellia Sinesis,* and belongs to family Theaceai. A huge fraction of tea waste is generated from tea processing factories and its disposal is a matter of concern. Waste tea could be a better adsorbent due to its easy availability (Amarasinghe and Williams, 2007; Wen et al., 2017; Liu et al., 2018; Pal and Maiti, 2019). Therefore, tea leaves waste may be used to synthesize tea based nanocomposites.

In this work silica was loaded on tea waste, here silica is used to enhance the adsorption capacity of tea leaves waste because of abundant hydroxyl groups present on its surface. Also, tea waste is used as a green reducing agent to switch the present work towards green approach. The cell wall of tea leaves is made up of carbohydrates, cellulose and lignin having diverse chemical moieties such as hydroxyl, phenolic, amine and carboxylic which interact with Pb^{2+} and Cd^{2+} ions by various processes including ion exchange and complex formation and can be used as bioadsorbent for metal ions recovery from wastewater (Weng et al., 2013). Since SiO_2@TW nanocomposites consist of amorphous silica nanoparticles which are loaded on tea waste that is an organic matter, so obtained materials was also an amorphous substances with abundant active sites and enhanced surface area, which make them good adsorbents (Cai et al., 2015a, 2015b). Therefore, SiO_2 loaded tea waste could be a capable sorbent for the recovery of Pb^{2+} and Cd^{2+} metal ions from wastewater. Keeping this in view, experiments were conducted on the fabrication of SiO_2 loaded tea waste nanocomposites and their application for lead and cadmium recovery from water.

2. Experiments

2.1. Materials

AR grade Cadmium nitrate tetrahydrate [$Cd(NO_3)_2.4H_2O$], Liquor ammonia, Lead nitrate [$Pb(NO_3)_2$] and Tetraethyl orthosilicate [$C_8H_{20}O_4Si$] have been used in this study.

2.2. Adsorbent fabrication process

2.2.1. Preparation of tea waste (TW)

Waste tea leaves were obtained from a factory and then cleaned and rinsed several times with Millipore water to pull out the dissolved impurities. After drying at 80 °C for 12 h, waste tea leaves were powdered and sieved using 1.40 mm mesh size sieve. The powdered waste tea leaves were kept in muffle furnace at 100 °C for 60 min. The prepared waste tea adsorbent was stored in airtight polybags and kept in desiccators for further use.

2.2.2. Fabrication of silica (SiO_2) nanoparticles

The nanoparticles of silica were fabricated by modified stober-method as earlier reported (Saini et al., 2018a, 2018b). In this procedure, absolute ethanol-water mixture 2:1(v/v) was mixed in ultra sonication bath for 15 min. After that 10 mL of liquor ammonia was added dropwise in this solution. To this reaction mixture 5 mL solution of tetraethoxysilane was added then it was sonicated for 1 h. The white colour gel so obtained was centrifuged, washed with millipore water and kept in hot air oven at 70 °C for 5 h to get silica nanoparticles. This silica nanoparticles powder was stored in plastic bottles for further use.

2.3. Synthesis of SiO_2@TW nanocomposites

To millipore water, 1.5 g of waste tea leaves was added with uninterrupted stirring for 10 min. Thereafter, 3.0 g of prepared silica nanopowder was dispersed into waste tea leaves solution and stirred for 30 min at room temperature (25 ± 1°C). This suspension was kept in sonicator for 1 h. The turbid substance so produced was centrifuged, washed and dried for 3 h at 80 °C in hot air oven. The resultant ash like product so produced was SiO_2@TW nanocomposites. Schematic diagram of synthesis of adsorbent is given in Fig. 1. Equation (1) represents the synthesis of silica nanoparticles and equation (2) represents the loading of silica nanoparticles on residual tea waste.

$$Si(OC_2H_5)_4 + 2\ H_2O \rightarrow SiO_2 + C_2H_5OH \qquad (1)$$

$$SiO_2 + TW \rightarrow TW - SiO_2 \qquad (2)$$

2.4. Characterization of adsorbents

The crystallinity of manufactured SiO_2@TW nanocomposites

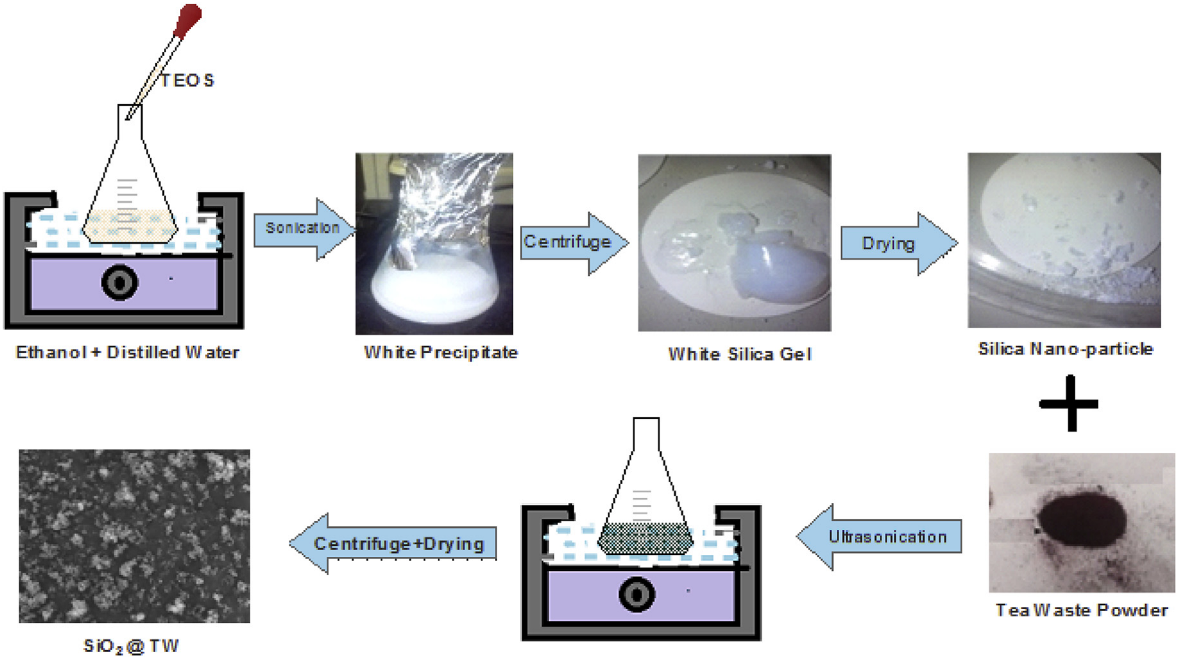

Fig. 1. Silica loaded tea waste nanocomposites synthesis by modified Stober method.

and residual tea adsorbent was examined by XRD technique using Rigaku miniflex II Diffractometer. Chemical functional groups were identified using SHIMADIZU IR AFFINITY-1 FTIR spectrophotometer. Energy-dispersive X-ray spectroscopy was employed for elemental arrangement and morphology of the adsorbents using Scanning electron microscope (SEM). Transmission electron microscopy (TEM) was used to explore the size of SiO_2@TW nanocomposites employing FEI Tecnai G^2 20 TWIN TEM (200 KV). The details of instruments used for characterization has already been reported by Joshi et al. (2019). BET analyzer (Quantachrome Instruments Nova, 2000e; USA) was employed to determine the surface area of synthesized adsorbents along with pore volume. Concentrations of Pb^{2+} and Cd^{2+} ions in solution were quantified by Flame Atomic Absorption Spectrophotometer (AAS) (GBC-SensAA, Australia).

2.5. Metal ions adsorption experiments

To evaluate the efficiency of SiO_2@TW nanocomposites and Residual tea waste adsorbent for removing the Pb^{2+} and Cd^{2+} ions from aqueous system, experiments were conducted in batch mode under different process conditions. Lead nitrate and cadmium nitrate tetrahydrate were used for the preparation of stock solutions of Pb^{2+} (1000 mg/L) and Cd^{2+} (1000 mg/L), in millipore water and working solutions were prepared. Known volumes of working solutions were agitated at 200 rpm after adding the adsorbent for predetermined time period. After achieving equilibrium, solution mixtures were centrifuged and residual Pb^{2+} and Cd^{2+} concentrations in supernatant were quantified using Atomic Absorption Spectrophotometer (GBC sensAA). The removal of metal ions and metal uptake capacity were determined following the equations given below.

$$\text{Metal ion removal }(\%) = \frac{(C_o - C_e)}{C_o} \times 100 \tag{3}$$

$$\text{Adsorption capacity at equilibrium}(q_e) = \frac{(C_o - C_e)\,V}{m} \tag{4}$$

Where, C_o (mg/L), and C_e (mg/L) are the initial and final metal ions concentration, m(g) denotes the adsorbent mass, V (L) denotes the volume of metal ions and q_e (mg/g) denotes the uptake capacity of adsorbents at equilibrium.

2.6. Reuse potential

Reusability is important to evaluate the efficiency of adsorbents as eco-friendly and sustainable approach. In this study, the regeneration and desorption of adsorbent was performed using HCl (0.1 M) as the desorbing agent in Erlenmeyer flasks by shaking it for 2 h at room temperature. The metal ions loaded SiO_2@TW and waste tea adsorbent were separated from metal ion solutions by centrifugation. Each adsorbent was treated using 50 mL solution of HCl (0.1 M), and then it was washed several times using millipore water and put in hot air oven at 100 °C for drying for 1 h. The reuse efficiency of SiO_2@TW nanocomposites and Tea waste adsorbent were determined for five cycles.

3. Results and discussion

3.1. Characterization of SiO_2@TW nanocomposites

The XRD analysis confirmed that the Silica nanoparticles, synthesized by modified stober method, are amorphous in nature. In the XRD spectrum of tea waste, two distinct peaks were observed at 24.24° and 29.62° and few short peaks were observed at 43.08° and 33.46° which indicated the presence of impurities with the organic tea waste. Since tea waste is a organic material, hence XRD pattern mostly shows the amorphous nature in the form of noise [Fig. 2a]. In XRD of Silica, broad hump between 20° and 30° suggested the amorphous nature of silica (Joshi et al., 2018) but when this silica is entrapped into tea waste surface (SiO_2@TW) then low intensity peaks were observed between 26.74° and 35.98° along with peak of

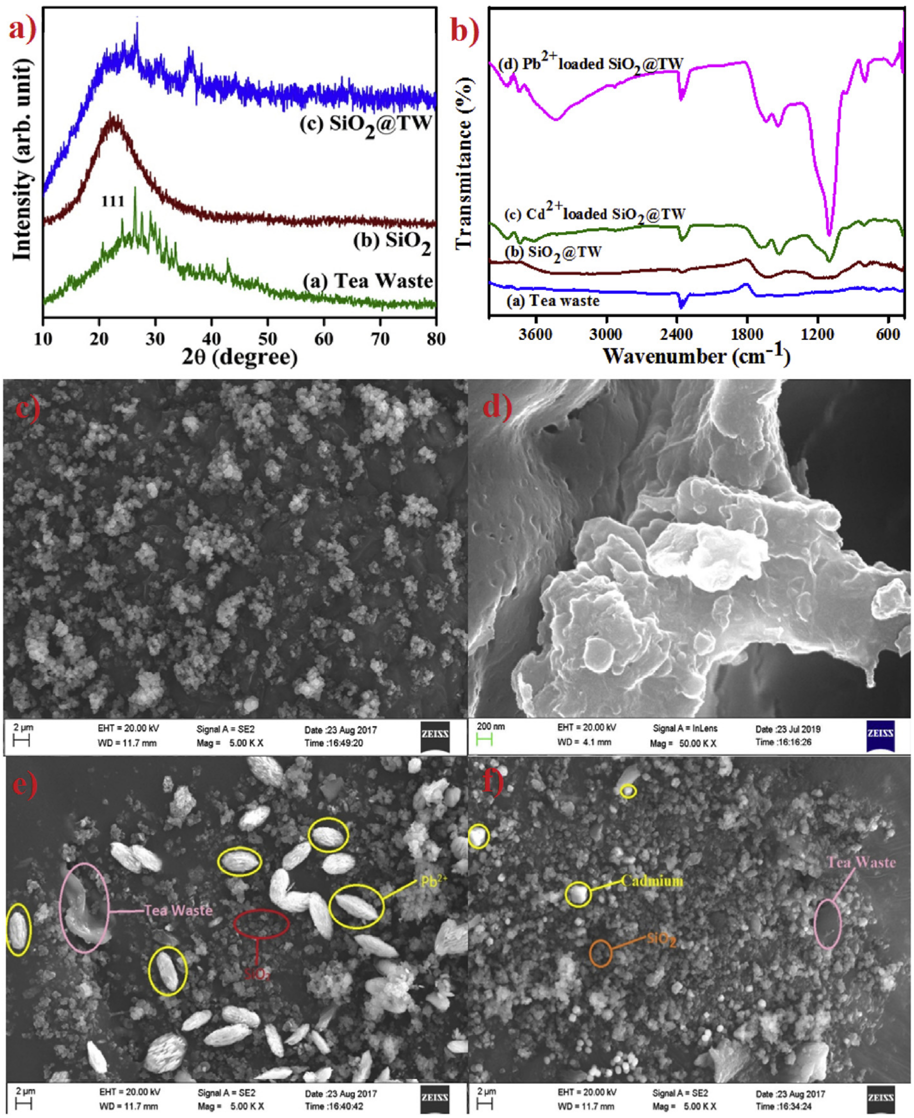

Fig. 2. (a) XRD spectra of tea waste, SiO$_2$ and prepared SiO$_2$@TW (b) FTIR spectra of Tea waste, SiO$_2$@TW, SiO$_2$@TW loaded with Cd^{2+} and Pb $^{2+}$ (c) FESEM images of SiO$_2$ @TW. (d) FESEM images of Tea waste, (e) FESEM images of Pb^{2+} loaded SiO$_2$@TW and (f) FESEM images of Cd^{2+} loaded SiO$_2$@TW.

silica [Fig. 2a]. Similar findings have been reported by Cai et al., 2015a, 2015b.

The morphological features of tea waste (TW) and SiO$_2$@TW nanocomposites, before and after adsorption, were characterized using SEM and TEM. In Fig. 2d, SEM image of tea waste shows that this material has uneven, irregular and rougher surface but somewhat fibrous because tea leave wastes are basically cellulose and having tannin and lignin organic components. Similarly, SEM micrographs of SiO$_2$@TW, before and after Pb^{2+} and Cd^{2+} adsorption, as shown in Fig. 2e and f. It is evident from Fig. 2c that SiO$_2$ appearance is like blossoms which are arranged in well organized pattern and distributed on the tea waste (TW) surface. Morphology of SiO$_2$ nanoparticles was slightly changed after incorporation of tea waste which is visible in SEM images. This indicates that SiO$_2$@TW had been synthesized successfully. Morphology of SiO$_2$@TW was also assessed after loading of Pb^{2+} and Cd^{2+}, it shows the entrapping of Cd^{2+} ions by bright coloured sugar cube like structures on the surface of nanocomposites. Similarly, Fig. 2e shows the grain like structures on the surface of SiO$_2$@TW nanocomposites due to the adsorption of Pb^{2+} ions and suggesting thereby the adsorption of metal ions onto SiO$_2$@TW nanocomposites.

To investigate elemental composition of SiO$_2$@TW, before and after Pb^{2+} and Cd^{2+} ions adsorption onto SiO$_2$@TW, EDX analysis was performed. In SiO$_2$@TW nanocomposites and Pb^{2+} and Cd^{2+} ions loaded SiO$_2$@TW nanocomposites, the weight percentage of detected elements are shown in Fig. 3a–d. The EDX spectra of Pb^{2+} and Cd^{2+} ions adsorption indicate that SiO$_2$@TW nanocomposites had the distinct peaks associated with Pb^{2+} and Cd^{2+} ions, thus identified the possible metal ions adsorption occurrence onto SiO$_2$@TW surface.

The particle size of SiO$_2$@TW nanocomposites was determined by TEM micrograph and the size of desired adsorbent was in the range of 6.8 nm–12 nm [Fig. 3e and f]. The selected area electron diffraction pattern (SAED) revealed the amorphous nature of the prepared material. This may be due to silica oxide and tea waste which is composed of organic matter and it was confirmed from the bright ball like TEM image that SiO$_2$@TW nanocomposites are amorphous in nature.

FTIR spectroscopy was employed to analyze the surface

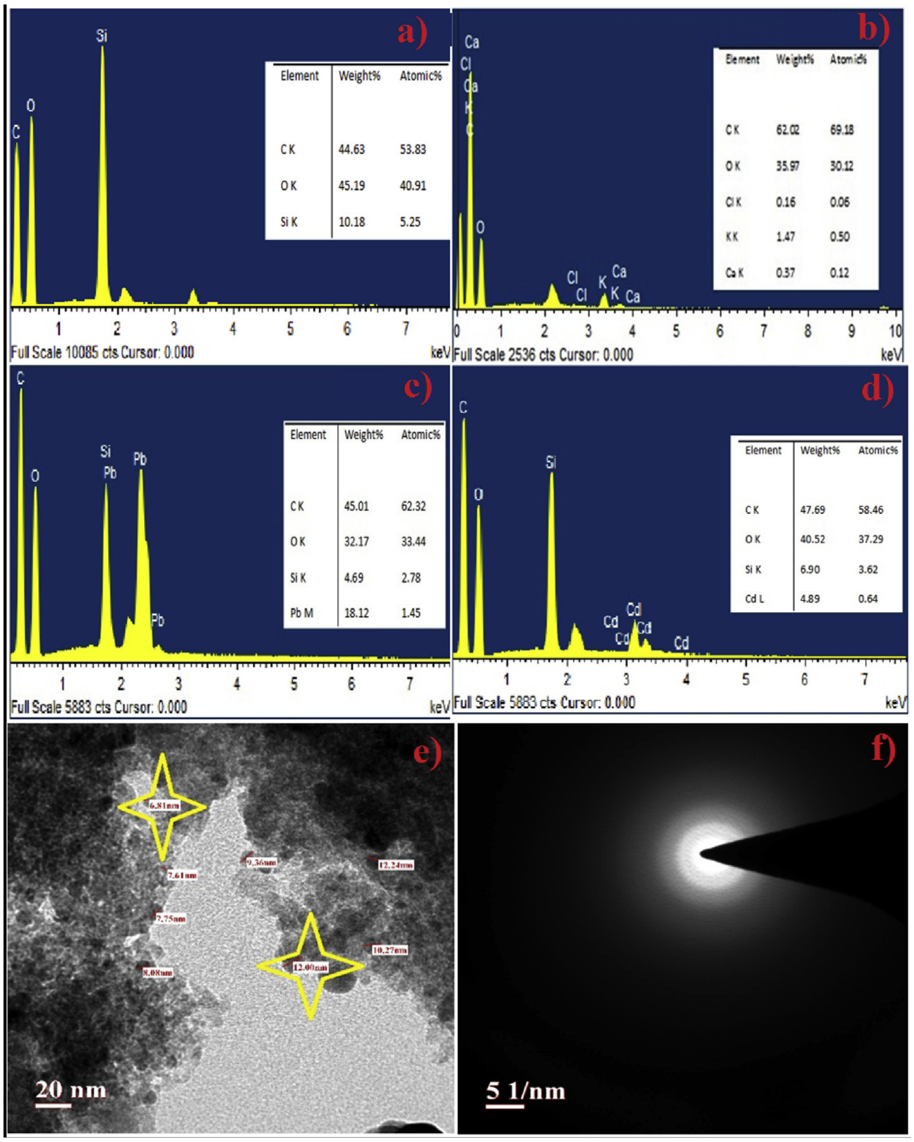

a)

Element	Weight%	Atomic%
C K	44.63	53.83
O K	45.19	40.91
Si K	10.18	5.25

b)

Element	Weight%	Atomic%
C K	62.02	69.18
O K	35.97	30.12
Cl K	0.16	0.06
K K	1.47	0.50
Ca K	0.37	0.12

c)

Element	Weight%	Atomic%
C K	45.01	62.32
O K	32.17	33.44
Si K	4.69	2.78
Pb M	18.12	1.45

d)

Element	Weight%	Atomic%
C K	47.69	58.46
O K	40.52	37.29
Si K	6.90	3.62
Cd L	4.89	0.64

Fig. 3. (a) EDX spectra of SiO_2@TW, (b) Tea waste, (c–d) SiO_2@TW loaded Pb^{2+} and Cd^{2+}respectively and (e) HRTEM Image of SiO_2@TW and (f) Selected area electron diffraction (SAED) pattern of SiO_2@TW

functional groups on the prepared nanoadsorbent. FTIR spectra of Tea waste (TW), SiO_2@TW, Pb^{2+} loaded and Cd^{2+} loaded SiO_2@TW are shown in Fig. 2b. In FTIR spectra of tea waste, small peak at 1709 cm^{-1} is attributed to C=O stretching of aldehyde group, some additional small peaks were also observed between 400 and 800 cm^{-1} that are due to the presence of impurities (Pirbazari et al., 2015). In IR spectra of SiO_2@TW, a peak between 491 and 493 cm^{-1} is associated with Si—O— Si bending mode of vibration. The IR band between 781-783 cm^{-1} may be assigned to symmetric stretching of Si—O— Si bonds. The adsorption peak observed at 1632 cm^{-1} is due to —OH binding vibration of H_2O molecules. The adsorption peak at 1212 cm^{-1} is due to C—N stretching. A strong peak at 1080 cm^{-1} relates the asymmetric stretching of Si—O—Si bond. Further, IR bands at 3200-3479 cm^{-1} are attributed to bending vibrations and stretching vibrations of O—H and Si—O—H bonds in surface water molecules. After adsorption of both the metal ions onto SiO_2@TW surface, some significant spectral changes were observed due to retention of metal ions. Some other peak was observed at 792 cm^{-1} in the FTIR spectra of Cd^{2+} ions loaded SiO_2@TW. In the Pb^{2+} loaded spectra peaks were observed at 812 cm^{-1} and 560 cm^{-1}. The IR band at 1530 cm^{-1} is due to secondary amine groups and at 2358 cm^{-1} is associated to amine —NH group (Fan et al., 2017; Pirbazari et al., 2015).

BET specific surface area of tea waste was 0.73 m^2/g and BJH total pore volume and diameter were near 0.002 cm^3/g and 9.74 nm, respectively. The surface area of synthesized SiO_2@TW nanocomposites was 9.86 m^2/g and that is higher than the raw tea waste. BJH pore volume was 0.024 cm^3/g and pore diameter was 9.61 nm, for SiO_2@TW. These results indicated that the pore size and surface area of SiO_2@TW nanocomposites were enhanced after the coating of SiO_2 nanoparticles as compare to raw tea waste. Similar observation has been reported by other authors (Fan et al., 2017) i.e., the specific surface area of raw tea waste was 0.913 m^2/g and its pore volume and average pore diameter were 0.007 cm^3/g and 2.6 nm, respectively. After loading of SiO_2 nanoparticles onto residual tea, pore volume and surface area of SiO_2@TW nanocomposites were enhanced.

3.2. *Batch mode adsorption studies*

3.2.1. *1. Effects of pH on metal ions sequestration*

Adsorption studies were performed to investigate the pH effect on both the metal ions P removal by SiO_2@TW nanocomposites and Tea waste adsorbent in the pH range, 2 to 8, by keeping other parameters constant. It was observed that removal of Pb^{2+} and Cd^{2+} ions increased as pH was increased 2 to 8 [Fig. 4a and b]. With residual tea waste adsorbent, removal of Pb^{2+} and Cd^{2+} ions was 9.88% and 17.8% at pH 2 and at pH 8 removal was 70.2% for Pb^{2+} ions and 77.38% for Cd^{2+} ions. Whereas SiO_2@TW nanocomposites were capable to remove Pb^{2+} and Cd^{2+} ions by 20% and 21.96% at pH 2 and at pH 8 removal was 89.82% of Pb^{2+} ions and 95.38% of Cd^{2+} ions. It is evident from the results that removal of metal ions increased with increased in pH from 2 to 8. The adsorption capacity of SiO_2@TW at pH 2 was 16.6 mg/g for Pb^{2+} ions and it became 74.4 mg/g at pH 6. Same trend was observed for Cd^{2+} removal by SiO_2@TW. The adsorption capacity of SiO_2@TW for Cd^{2+} was 18.3 mg/g at pH 2 and it became 79.48 mg/g at pH 8. Lesser adsorption at lower pH may be associated to the competition for adsorption sites among H^+ ions and metal ions. Sometimes, protons present on functional groups of adsorbents results in repulsion of metal ions in acidic conditions. In alkaline conditions, due to enhancement of negative charge in metal ion solutions there may

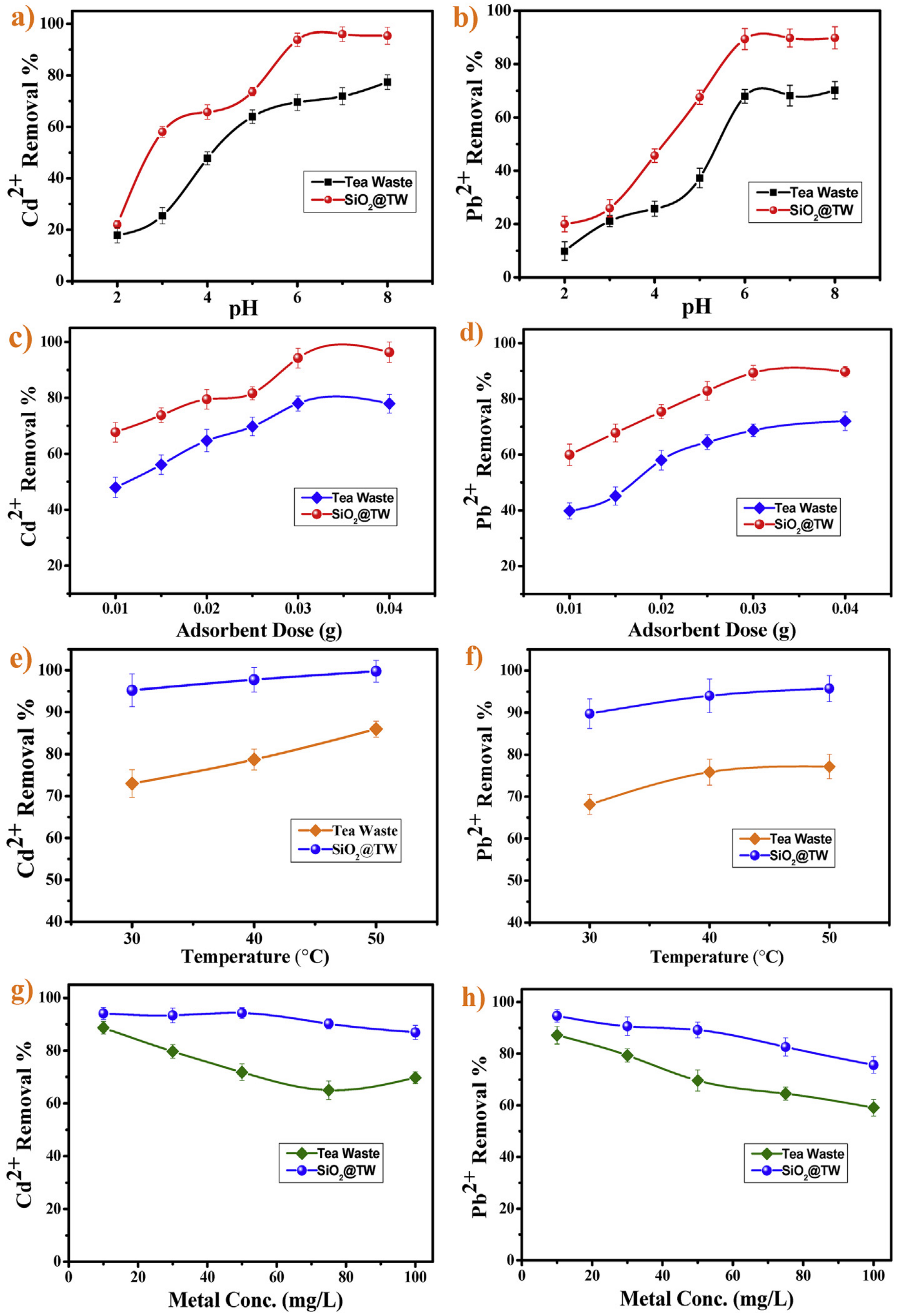

Fig. 4. (a) Effect of pH on Cd^{2+} removal, (b) Effect of pH on Pb $^{2+}$ removal, (c) Effect of adsorbent dose on Cd^{2+} removal, (d) Effect of adsorbent dose on Pb^{2+} removal, (e) Effect of temperature on Cd^{2+} removal and (f) Effect of temperature on Pb^{2+} removal (g) Effect of concentration on Cd^{2+} removal (h) Effect of concentration on Pb^{2+} removal.

be electrostatic attraction among the anionic adsorbent surface and cationic metal ions, thus at higher pH, deprotonation of different functional groups such as phenols, carboxylic and alcohols take place. Beyond pH 6 (for Pb^{2+}) and pH 8 (for Cd^{2+}), metal ions are hydrolyzed to hydroxide forms and they get precipitated (Mohammed, 2012; Kataria and Garg, 2018a). Hence it can be concluded that adsorption of metal ions was influenced by pH due to the competition for adsorption sites among metal ions and H^+ ions present in the solution (Iqbal et al., 2009). For further experiments the pH was optimized at pH 6 and pH 7 for the removal of Pb^{2+} and Cd^{2+} ions, respectively.

3.2.2. Effects of adsorbent quantity on metal ions sequestration

Fig. 4c and d represent the removal of Pb^{2+} and Cd^{2+} ions with respect to dose of SiO_2@TW and Tea waste adsorbent in the range 0.01–0.04 g/50 mL of solution at pH 6 for Pb^{2+} ions and at pH 7 for Cd^{2+} ions . It is evident from the results that the removal of both the metal ions (Pb^{2+} and Cd^{2+} ions) by both the adsorbents increased with adsorbent dose. In case of tea waste adsorbent removal of Pb^{2+} ions increased from 39.8 to 72% and for Cd^{2+} ions it increased from 47.94 to 72.14%. Similar trend was observed with SiO_2@TW nanocomposites, removal of Pb^{2+} ions increased from 59.94 to 89.76% and for Cd^{2+} ions it increased from 67.72% to 96.34%. This increase in metal ions removal with adsorbent dose may be associated to enhanced availability of surface area and adsorption sites on the adsorbents (Thakur and Parmar, 2013). The result shows that metals removal efficiency of SiO_2@TW adsorbent was higher as compared to tea waste adsorbent. This may be due to the presence of additional functional groups and binding sites on the surface of SiO_2@TW nanocomposites.

3.2.3. Effect of temperature variation on metal ions removal

Temperature is an important parameter for the adsorption process because with increased temperature, mobility of ions increase and it also increase active sites onto adsorbent due to breaking of chemical bonds at elevated temperatures. Fig. 4e-f depict the adsorption of Pb^{2+} and Cd^{2+} metal ions onto SiO_2@TW nanocomposites and Tea waste adsorbent in the temperature range of 30 –50 °C. It was inferred that the removal of the Pb^{2+} and Cd^{2+} ions increased from 68.2% to 77.2% and 73% to 86%, respectively, when Tea waste adsorbent was used. Similarly when SiO_2@TW nanocomposites used as adsorbent then the removal of Pb^{2+} and Cd^{2+} ions increased from 89.8 to 95.7% and 95.2–99.7%, respectively. This is because at elevated temperature, the contact between metal ions with the adsorbents surface active sites is enhanced. Therefore, it leads to rise in transportation and diffusion of metal ions in solution because increased temperature acts as catalyst for adsorption process (Malkoc and Nuhoglu, 2007).

3.2.4. Effect of metal ions concentration on their removal

The Pb^{2+} and Cd^{2+} metal ions adsorption onto SiO_2@TW nanocomposites and Tea waste adsorbent were evaluated at different metal ions concentration (10, 30, 50, 75 and 100 mg/L) by keeping the remaining parameters unchanged (i.e. pH 6 for Pb^{2+} ions and pH 7 for Cd^{2+} ions, adsorbent dose of 0.03g, contact time 10–60 min, temperature 27 °C and stirring speed 200 rpm). The results showed that when tea waste adsorbent used there was a considerable decrease in percentage removal of Pb^{2+} ions (from 87 to 59.07%) and Cd^{2+} ions (from 88.7 to 69.7%) with increase in metal ions concentrations. Similarly, when SiO_2@TW nanocomposites used as adsorbent the removal of Pb^{2+} and Cd^{2+} ions decreases from 94.70 to 75.64% and 94.10 to 86.93% with increase in metal ions concentrations [Fig. 4(g-h)]. The possible reason for this may be due to non-availability of active sites for metal ions adsorption at higher concentrations (Gupta and Ali, 2000; Thakur and Parmar, 2013).

3.2.5. Effects of contact time on the removal of metals

The Pb^{2+} and Cd^{2+} ions removal by SiO_2@TW nanocomposites and tea waste adsorbent were evaluated at different contact times (10–60 min) by keeping the remaining parameters constant. The results revealed that initially there was a sharp rise in metal ions removal with time for both the adsorbents and then attains equilibrium. At 50 mg/L concentration, the maximum removal of Pb^{2+} and Cd^{2+} metal ions was 69.6% and 71% by tea waste adsorbent and then attained equilibrium (Fig. 5a-b). On the other hand, SiO_2@TW nanocomposites maximum removal of Pb^{2+} and Cd^{2+} metal ions was 89.22% and 94.28% and then attained equilibrium with time (Fig. 5c-d). This may be associated to the presence of numerous free active sites on the adsorbent surface initially than with time, the adsorption process slowed and attained equilibrium due to saturation of active sites on the adsorbent (Ahlawat et al., 2019).

3.3. Adsorption kinetic modeling

The Pseudo-first order (Langergren and Svenska, 1898) and pseudo-second order (Mckay and Ho, 1999) models were applied to determine the rate of adsorption of Pb^{2+} and Cd^{2+} ions onto SiO_2@TW nanocomposites and Tea waste adsorbent. The linear forms of both the models are presented in the following equations.

$$\log(q_e - q_t) = log q_e - \left(\frac{k_1}{2.303}\right)t \tag{5}$$

$$t \Big/ q_t = 1 \Big/ k_2\, q_e^2 + t \Big/ q_e \tag{6}$$

Where, q_e denotes the adsorption capacity (mg/g) of metal ions at equilibrium time, q_t denotes the metal ion uptake capacity (mg/g) at time t whereas, k_1 (min^{-1}) and k_2 g.$(mg.min)^{-1}$ denotes the pseudo-first and pseudo-second order kinetic rate constants, respectively.

The plot of pseudo-first order was drawn between log ($q_e - q_t$) *vs* t and the values of kinetic parameters i.e., $q_{e,}$ R^2 and k_1 were calculated. Similarly for pseudo-second order, the values of $q_{e,}$ k_2 and R^2 were calculated from the plot between t/q_t *vs* t. The calculated values are given in Table 1. For SiO_2@TW nanocomposites, the values of regression coefficients (R^2) in Pseudo-second order is varied from 0.974 to 0.996 for Pb^{2+} and 0.965 to 0.998 for Cd^{2+} ion which is greater than Pseudo-first order regression coefficient (R^2). The qe (calculated) values of pseudo-second order model are also near to the qe (experimental) values for both the metal ions. Therefore, pseudo-second order model is found to be best fitted and main adsorption rate controlling factor for metal ion uptake by SiO_2@TW nanocomposites. While in case of tea waste, opposite trend was noticed in the adsorption of both the metal ions. Here Pseudo-first order regression coefficient is greater than that of Pseudo-second order regression coefficient suggesting the good agreement of Pseudo-first order rate model (El Azazy et al., 2019; He et al., 2016) Table 1.

The kinetic data of adsorption by tea waste revealed that Pseudo-first order is best fitted, which indicated the involvement of physical adsorption. From the SEM images, it was confirmed that the morphology of adsorbent surface is porous; due to this metal ions are adsorbed on the surface as well as in the pores of the adsorbent. This indicates the physical adsorption of metal ions onto tea waste.

3.4. Isotherm modelling

The Langmuir, Freundlich, Temkin, and Dubinin-Radushkevich isotherm models were employed to explore the adsorption

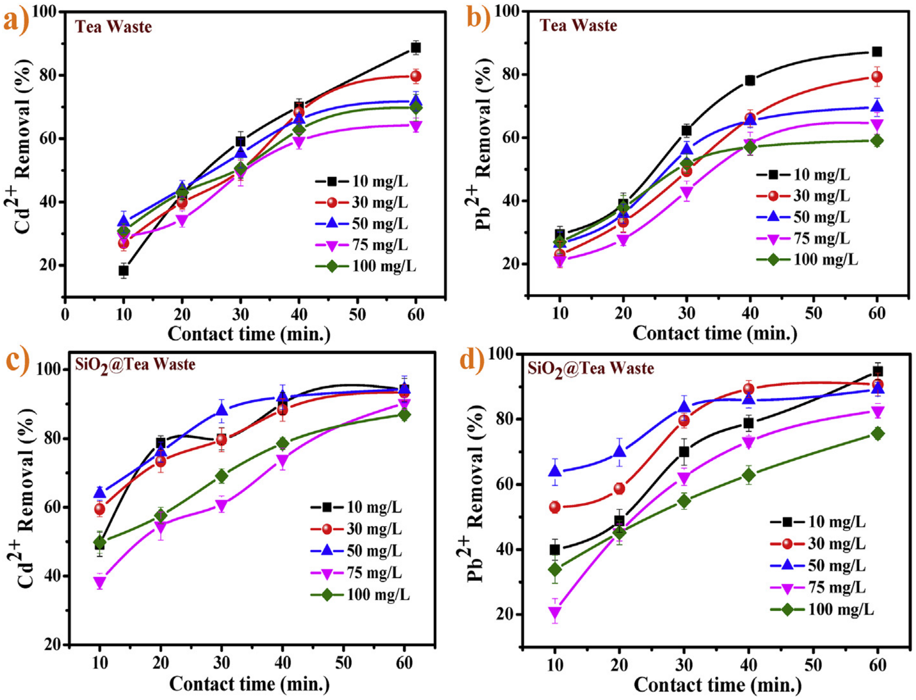

Fig. 5. (a) Effect of contact time on Cd^{2+} removal onto tea waste, (b) Effect of contact time on Pb^{2+} removal onto tea waste (c) Effect of contact time on Cd^{2+} removal onto SiO$_2$@TW, (d) Effect of contact time on Pb^{2+} removal onto SiO$_2$@TW.

Table 1
Kinetic models parameters for Pb^{2+} and Cd^{2+}adsorption onto Tea Waste adsorbent and SiO$_2$@TW nanocomposites.

Adsorbents			Tea Waste adsorbent							SiO$_2$@TW nanocomposites					
Metal	Conc. (mg/L)	q_e (exp.)	Pseudo-first order			Pseudo-second order			q_e (exp)	Pseudo-first order			Pseudo-second order		
			k_1 (min^{-1})	q_e (cal)	R^2	k_2 (gmg^{-1} min^{-1})	q_e (cal)	R^2		k_1 (min^{-1})	q_e (cal)	R^2	k_2 (gmg $^{-1}$ min^{-1})	q_e (cal)	R^2
Pb^{2+}	10	14.5	0.050	17.2	0.931	0.0007	28.2	0.846	15.8	0.046	16.4	0.987	0.0017	22.2	0.989
	30	39.7	0.068	81.8	0.943	0.0001	91.7	0.842	45.3	0.070	39.0	0.781	0.0013	56.5	0.974
	50	58	0.077	111.2	0.934	0.0003	97.1	0.898	74.4	0.065	42.5	0.967	0.0019	82.6	0.996
	75	80.7	0.084	202.6	0.945	0.0001	166.7	0.802	103.3	0.087	258.2	0.960	0.0002	172.4	0.985
	100	98.5	0.085	143.8	0.979	0.0004	133.3	0.979	126.1	0.083	274.7	0.876	0.0002	172.4	0.981
Cd^{2+}	10	14.8	0.584	24.5	0.946	0.0001	51.3	0.644	15.7	0.540	9.94	0.816	0.0048	18.8	0.992
	30	39.9	0.067	72.9	0.945	0.0003	71.4	0.928	46.7	0.058	32.04	0.983	0.0021	53.2	0.998
	50	59.8	0.072	91.0	0.952	0.0006	81.3	0.969	78.6	0.069	47.20	0.950	0.0017	87.7	0.998
	75	80.4	0.080	145.7	0.962	0.0003	117.6	0.945	112.8	0.081	249.29	0.865	0.0002	156.2	0.965
	100	116.3	0.084	237.8	0.931	0.0003	161.3	0.984	144.9	0.083	237.30	0.918	0.0004	175.4	0.987

behaviour or interaction between metal ions with surface of adsorbents. The Langmuir equation is given below (Langmuir, 1916, 1918):

$$\frac{C_e}{q_e} = \frac{1}{q_{max} b} + \frac{C_e}{q_{max}} \tag{7}$$

Where, q_{max} denotes the maximum adsorption capacity (mg/g) of metal ions, *b* denotes the Langmuir constant (L/mg). The values of adsorption model parameters were obtained from the linear plot of Ce/qe *versus* Ce. The values of Langmuir parameter (q_{max}), constant (b) and correlation coefficient (R^2) for both the metals onto Tea waste adsorbent and SiO$_2$@TW nanocomposites are given in Table 2.

The linear form of Freundlich isotherm model is given below:

$$log q_e = log K_f + \frac{1}{n} log C_e \tag{8}$$

Table 2
Adsorption isotherms parameters for Pb^{2+}and Cd^{2+} adsorption on Tea Waste and SiO$_2$@Tea Waste.

Isotherms model	Parameters	Tea Waste		SiO$_2$@Tea Waste	
		Pb^{2+}	Cd^{2+}	Pb^{2+}	Cd^{2+}
Langmuir	q_{max} (mg/g)	125.0	142.9	153.8	222.2
	b (L/mg)	0.076	0.069	0.173	0.144
	R^2	0.965	0.820	0.993	0.963
Freundlich	n	1.823	1.714	1.81	1.40
	K_f (mg/g)	13.29	13.62	24.62	27.31
	R^2	0.995	0.983	0.979	0.949
Temkin	B	106.33	95.41	85.164	59.138
	K_T (L/mg)	1.136	1.117	2.518	2.088
	R^2	0.950	0.840	0.970	0.975
Dubinin- Radushkevich	Q_s (mg/g)	68.09	71.46	86.46	103.23
	K_D (mol^2/kJ^2)	0.0008	0.0006	0.0002	0.0003
	E (kJ/mol)	25.0	28.9	50	40.8
	R^2	0.834	0.791	0.839	0.883

Where n denotes the heterogeneity factor and K_f denotes the Freundlich constant. The linear plot between log qe vs log Ce was employed to determine the values of parameters. The value of n should be $1 < n < 10$ for favorable adsorption.

The linear form of Temkin isotherm model is expressed in equation (9) (Temkin and Pyzhe, 1940):

$$q_e = BlnKT + BlnC_e \tag{9}$$

where $B = RT/b$, and b denotes the Temkin constant explaining the heat of adsorption, R denotes the universal gas constant, T denotes the temperature and KT (L/g) is equilibrium binding constant. The Temkin parameter values were evaluated by plotting graph among q_e vs $ln\ C_e$. The values of $R^2$and other parameters for both the metals are given in Table 2.

Dubinin-Radushkevich isotherms (DR) model (Dubinin and Radushkevich, 1947) is given in equation (10):

$$lnq_e = lnQs - K_D\varepsilon^2 \tag{10}$$

$$\varepsilon = RT\ \mathrm{In}(1 + 1/\mathrm{C_e}) \tag{11}$$

Where, Qs denotes the maximum adsorption capacity (mg/g), ε is Polanyi potential, K_D (mol^2/kJ^2) is the activity coefficient (mean adsorption energy). The values of K_D and Qs were calculated from the slope and intercept determined by plotting graph among $ln\ q_e$ versus ε. The mean adsorption energy E (kJ/mol) was determined from the equation given below.

$$E = 1\Big/\sqrt{2K_D} \tag{12}$$

The D-R model was implemented to the experimental data of both the metals onto Tea waste adsorbent and SiO_2@TW nanocomposites to evaluate the characteristics of adsorbents and mean free energy. The correlation coefficient and parameters related to D-R model are provided in Table 2.

After evaluating the adsorption isotherm models, it was found that the Langmuir isotherm model is best fitted to the experimental data for the adsorption of Pb^{2+} and Cd^{2+} ions onto SiO_2@TW nanocomposites. Whereas in case of tea waste adsorbent, Freundlich isotherm model was found to be best fitted than remaining isothermal models studied in the present work. The obtained value of R_L was found to lie between 0 and 1 ($0< R_L < 1$) indicated Pb^{2+} and Cd^{2+} adsorption onto SiO_2@TW nanocomposites is favorable. For both the metal ions, obtained value of n was more than 1 which signifies the multilayer adsorption on the heterogeneously distributed active sites of both the adsorbents. A comparison of maximum adsorption capacity of earlier reported adsorbent with SiO_2@TW and tea waste adsorbent is given in Table 3. It illustrated that SiO_2@TW nanocomposites have adsorption capacity more than the tea waste and other reported adsorbents. Therefore, it was concluded that SiO_2@TW nanocomposites could be a good adsorbent for the removal of metal ions from aqueous system.

3.5. Thermodynamic studies

The information regarding Gibb's free energy (ΔG^0), change in entropy (ΔS^0) and enthalpy (ΔH^0) for the Pb^{2+} and Cd^{2+} adsorption onto SiO_2@TW nanocomposites and tea waste was determined by performing experiments at various temperatures in the range of 30–50 °C by keeping all the parameters constant. Following equations were used to calculate the different thermodynamic parameters (Smith and Ness, 1987):

$$\varDelta G^0 = -RTlnK_d \tag{13}$$

$$K_d = \frac{C_a}{C_e} \tag{14}$$

$$lnK_d = -\frac{\Delta H^0}{RT} + \frac{\Delta S^0}{R} \tag{15}$$

Where, R is gas constant (8.314 J $mol^{-1}K^{-1}$), K_d is equilibrium constant, temperature (K) is denoted by T and C_a (mg/L) denotes the quantity of metal ions on the surface of adsorbent at equilibrium. The values of slope and intercept were obtained after drawing linear plots between ln K_d *Vs* 1/T, which is used for calculating ΔH° and ΔS°. The thermodynamic parameters are presented in Table 4. The positive values of ΔS° for both the metal ions during adsorption onto Tea waste and SiO_2@TW nanocomposites verified the increase in degree of randomness at the solid-solution interface. In addition, the positive values of ΔH° for Pb^{2+} and Cd^{2+} ions by both the adsorbent showed that the process of adsorption is endothermic in nature and the ions were absorbed on the surface of adsorbent. For both the adsorbents, negative ΔG° values for Pb^{2+} and Cd^{2+} at higher temperatures verified the feasibility as well as spontaneity of adsorption process and suggests the physical adsorption of both the metal ions by both the adsorbents (Malkoc and Nuhoglu, 2007).

3.6. Reuse potential of the nanocomposite for metal removal

The regenerated SiO_2@TW and Tea waste adsorbent were used for adsorption of both the metal ions up to five reuse cycles. In the first round of SiO_2@TW nanocomposites, the removal for Pb^{2+} and Cd^{2+} ions was 67.3% and 77.9% respectively that was greater than the Tea waste adsorbent. But in next round, the removal efficiency for both the metal ions was significantly decreased and at the end of fifth round it was only 55% for Pb^{2+} and 51.8% for Cd^{2+} ions (Fig. 6). This study suggests that both the adsorbent have potential to remove the metal ions from aqueous solutions during reuse but it decreases with each use.

3.7. Adsorption mechanism

Four different reaction mechanisms viz., surface charge, formation of covalent bonds, cation- π interaction and ion exchange played important role in the adsorption of metal ions. Adsorption process may be chemical or physical depending on the chemistry of adsorbent and adsorbate. The variation in pH of the solution alters the solvation process of hydrogen (H^+), hydronium (H_3O^+) and hydroxyl (OH^-) ions in aqueous system which affects the surface charge of the adsorbent and chemical nature of metal ions. 3.1 FTIR spectra confirmed that the surface of SiO_2@TW nanocomposites contained oxy (SiO^-) and carboxyl ($COO{-}H^+$) groups that involved in the adsorption of Pb^{2+} and Cd^{2+} ions. Both metals ions are divalent in nature and contain positive charge. These metal ions adsorbed on the surface of SiO_2@TW nanocomposites by electrostatic interaction between divalent metal ions and oxygen containing groups such as $Si{-}O^-$,$OH{-}$ COO^-. The broad band from 3500 to 3300 cm^{-1} and sharp absorption peak at 1080 cm^{-1} observed after Pb^{2+} adsorption in FTIR spectra indicated that Pb^{2+} could be adsorbed on adsorbent surface as $Pb(OH)_2$ and $Pb{-}S{=}O$, respectively. FTIR spectra results also indicated that $Si{-}O$ and $O{-}H$ groups of SiO_2@TW bound with the Pb^{2+} as well as Cd^{2+} ions by electrostatic interactions and also the available functional groups in adsorbent can bind via cation-π interactions. The absorption peak

Table 3
Comparison of the adsorption capacity of synthesized adsorbent for Pb^{2+} and Cd^{2+} removal with other reported adsorbents.

Adsorbents	Metals	Q_{max} (mg/g)	pH	Fit isotherm	References
Tea waste	Pb^{2+}	65	5.5	Freundlich	Amarasinghe and Williams (2007)
magnetic chrysotile nanotubes	Pb^{2+}	27.64	5	Langmuir	Yu et al. (2015)
SiO_2@OPW	Pb^{2+}	200	6	Langmuir	Saini et al., (2018a)
multi-metal binding biosorbent	Pb^{2+2+}	76.25	5.5	sips	Abdolali et al. (2016)
Mango peel waste	Pb^{2+}	99.05	5	Langmuir	Iqbal et al., 2009
Tea waste	Pb^{2+}	33.49	5	Langmuir	Wan et al. (2014)
Akali treated Tea waste	Pb^{2+}	64.1	4.5	Langmuir	Yang and Cui (2013)
Zno nanoparticles	Pb^{2+}	115	6	Freundlich	Kataria and Garg, (2018b)
Magnetic Chrysotile Nano Tube	Pb^{2+}	23.82	5.5	Langmuir	Yu et al. (2015)
SiO_2@TW	Pb^{2+}	153.8	6	Langmuir	This work
multi-metal binding biosorbent	Cd^{2+}	31.73	5.5	sips	Abdolali et al. (2016)
EDTA@Fe_3O_4/SC nanocomposites	Cd^{2+}	63	6.5	Langmuir	Kataria and Garg, (2018a)
Mixed maghemite-magnetite nanoparticles	Cd^{2+}	2.7	9.5	Langmuir	Chowdhury and Yanful (2013).
Zno nanoparticles	Cd^{2+}	71.5	6	Freundlich	Kataria and Garg, (2018b)
Mango peel waste	Cd^{2+}	68.92	5	Langmuir	Iqbal et al. (2009)
Tea waste	Cd^{2+}	16.87	5	Langmuir	Wan et al. (2014)
SiO_2@TW	Cd^{2+}	222.2	7	Langmuir	This work

Table 4
Thermodynamic parameter description for Pb^{2+} and Cd^{2+} adsorption on Tea Waste and SiO_2@Tea Waste.

Temp. (K)	Tea Waste adsorbent						SiO_2@TW nanocomposites					
	Pb^{2+}			Cd^{2+}			Pb^{2+}			Cd^{2+}		
	ΔG° (k J mol^{-1})	ΔS° (J $mol^{-1}K^{-1}$)	ΔH° (k J mol^{-1})	ΔG° (k J mol^{-1})	ΔS° (J $mol^{-1}K^{-1}$)	ΔH° (k J mol^{-1})	ΔG° (k J mol^{-1})	ΔS° (J $mol^{-1}K^{-1}$)	ΔH° (k J mol^{-1})	ΔG° (k J mol^{-1})	ΔS° (J $mol^{-1}K^{-1}$)	ΔH° (k J mol^{-1})
303	−1.92	211.19	63.74	−2.50	202.86	60.17	−5.47	219.75	61.91	−3.69	380.20	107.97
313	−2.98			−3.40			−7.17			−7.07		
323	−3.27			−4.87			−8.36			−8.36		

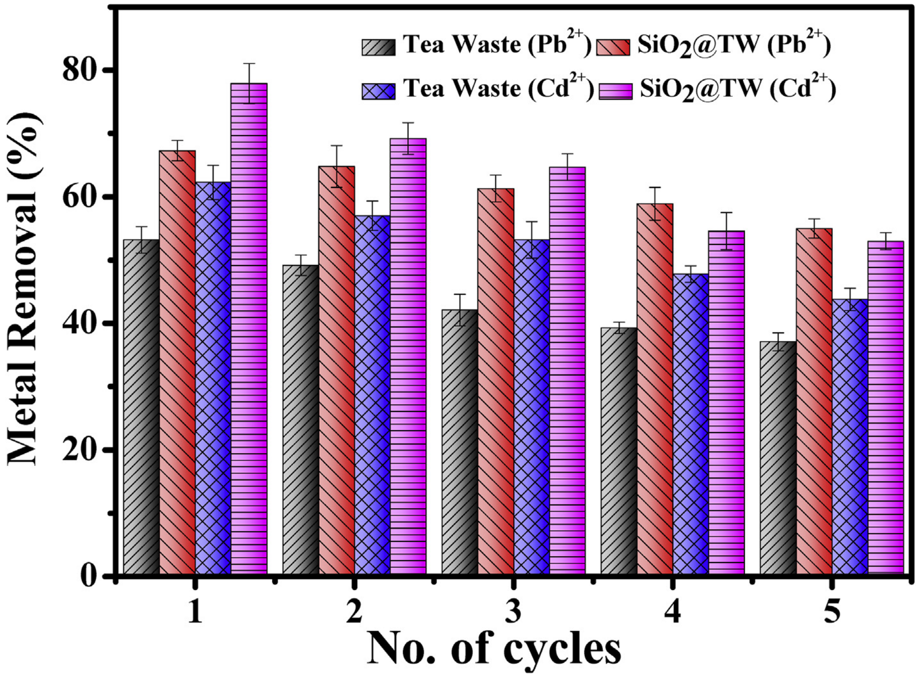

Fig. 6. Reusability potential of SiO_2@TW and Tea Waste adsorbent for $Cd^{2+}$and Pb^{2+}.

at 2380 cm^{-1} indicated that the amine group of tea waste adsorbent may be involved in the binding of Pb^{2+} and Cd^{2+} metal ions. The results of pH study also indicated that divalent metals ions electrostatically attract towards the surface of SiO_2@TW nanocomposite. The surface of adsorbents (SiO_2@TW and Tea Waste) contained hydrogen ion (H^+) at pH 6 that indicates ions exchange process may also be involved in adsorption of divalent ions onto adsorbent (Abdolali et al., 2016). Fig. 7 shows the possible adsorption mechanism for metal ions removal by SiO_2@TW.

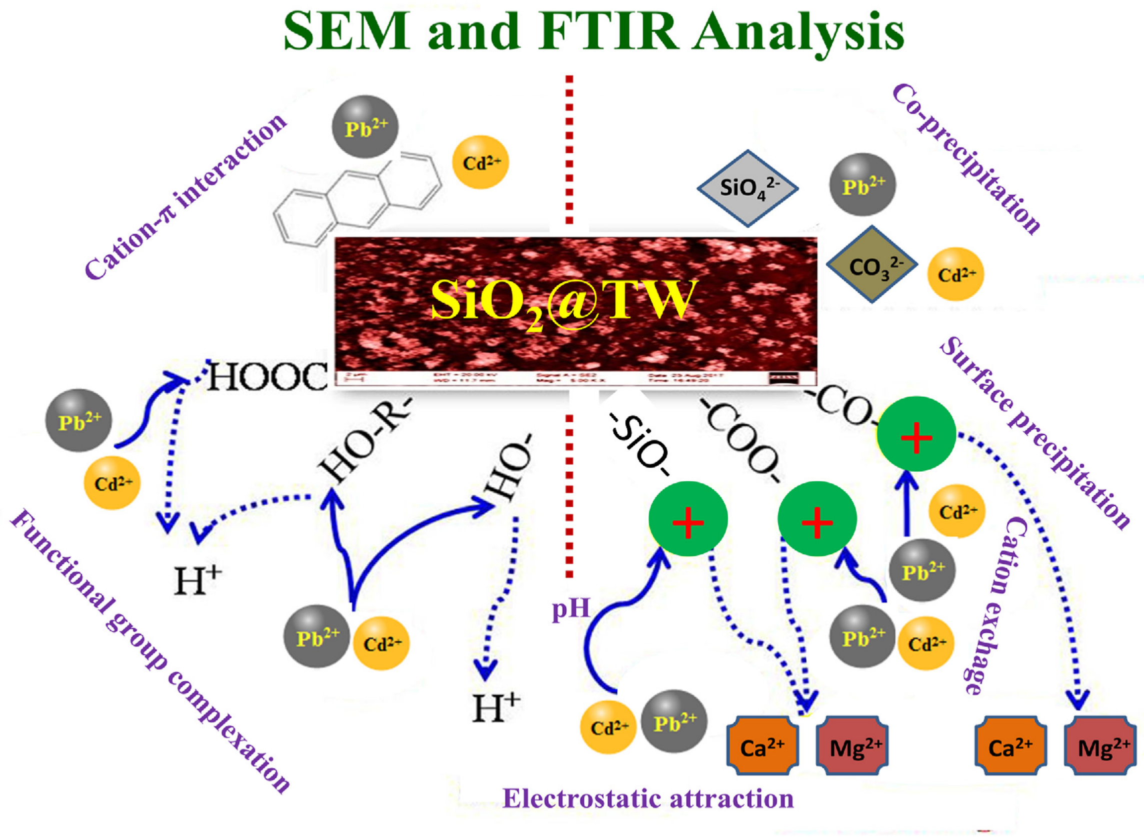

Fig. 7. Possible adsorption mechanism for metal ions removal onto SiO_2@TW nanocomposites

4. Conclusion

Based on the results it can be concluded that SiO_2@TW adsorbent is an efficient adsorbent for the removal of Pb^{2+} and Cd^{2+} metal ions from aqueous solutions. It has promising adsorption capacity under optimized process conditions. Tea waste has also been used as adsorbent for metal ions recovery from aqueous solution. This study revealed that tea waste exhibited promising Langmuir adsorption capacity for Pb^{2+} (125 mg/g) and Cd^{2+} (142.9 mg/g) metal ions but SiO_2@TW adsorbent is more efficient for the removal of metals from aqueous solution. The adsorption capacity of SiO_2@TW adsorbent for Pb^{2+} was 153 mg/g and for Cd^{2+} was 222.2 mg/g.

Declaration of competing interest

There are no conflicts to declare.

CRediT authorship contribution statement

Seema Joshi: Investigation, Writing - original draft. **Navish Kataria:** Supervision, Writing - review & editing. **V.K. Garg:** Resources, Supervision, Writing - review & editing. **K. Kadirvelu:** Formal analysis.

Acknowledgement

One of the authors Ms. Seema joshi is very thankful to University Grants Commission, New Delhi India for providing the financial support in the form of BSR-UGC Fellowship (as JRF and SRF). Authors are very thankful to the DRDO-BU Center for Life Sciences, Bharathiar University Campus, Coimbatore, Punjab University, Chandigarh and Central university of Punjab, Bathinda for providing the analytical facilities for the characterization of materials.

References

Abdolali, A., Ngo, H.H., Guo, W., Lu, S., Chen, S.S., Nguyen, N.C., Wu, Y., 2016. A breakthrough biosorbent in removing heavy metals: Equilibrium, kinetic, thermodynamic and mechanism analyses in a lab-scale study. Sci. Total Environ. 542, 603–611. https://doi.org/10.1016/j.scitotenv.2015.10.095.

Ahlawat, W., Kataria, N., Dilbaghi, N., Has san, A.A., Kumar, S., Kim, K.H., 2019. Carbonaceous nanomaterials as effective and efficient platforms for removal of dyes from aqueous systems. Environ. Res. 181, 108904, https://doi.org/10.1016/j.envres.2019.108904.

Amarasinghe, B.M.W.P.K., Williams, R.A., 2007. Tea waste as a low cost adsorbent for the removal of Cu and Pb from wastewater. Chem. Eng. J. 132, 299–309. https://doi.org/10.1016/j.cej.2007.01.016.

Bulgariu, L., Lupea, M., Bulgariu, D., Rusu, C., Macoveanu, M., 2013. Equilibrium study of Pb (II) and Cd(II) biosorption from aqueous solution on marine green algae biomass. Environ. Eng. Manag. J. 12, 183–190. https://doi.org/10.30638/eemj.2013.021.

Cai, H., Chen, G., Peng, C., Xu, L., Zhu, X., Zhang, Z., Wan, X., 2015a. Enhanced removal of fluoride by tea waste supported hydrous aluminium oxide nanoparticles: anionic polyacrylamide mediated aluminium assembly and adsorption mechanism. RSC Adv. 5, 29266–29275. https://doi.org/10.1039/C5RA01560J.

Cai, H., Chen, G., Peng, C., Zhang, Z., Dong, Y.Y., Shang, G.Z., Wan, X.C., 2015b. Removal of fluoride from drinking water using tea waste loaded with Al/Fe oxides: a novel, safe and efficient biosorbent. Appl. Surf. Sci. 328, 34–44. https://doi.org/10.1016/j.apsusc.2014.11.164.

Chauhan, A.K., Kataria, N., Garg, V.K., 2020. Green fabrication of ZnO nanoparticles using Eucalyptus spp. leaves extract and their application in wastewater remediation. Chemosphere 247, 125803. https://doi.org/10.1016/j.chemosphere.2019.125803.

Chowdhury, S.R., Yanful, E.K., 2013. Kinetics of cadmium (II) uptake by mixed maghemite-magnetite nanoparticles. J. Environ. Manag. 129, 642–651. https://doi.org/10.1016/j.jenvman.2013.08.028.

Dubinin, M.M., Radushkevich, L.V., 1947. The Equation of the characteristic curve of activated charcoal. Chem. Zentr. 1, 875–890.

El-Azazy, M., El-Shafie, A.S., Issa, A.A., Al-Sulaiti, M., Al-Yafie, J., Shomar, B., Al-Saad, K., 2019. Potato peels as an adsorbent for heavy metals from aqueous solutions: eco-structuring of a green adsorbent operating Plackett–Burman design. Int. J. Chem. 1–14. https://doi.org/10.1155/2019/4926240.

Fan, S., Wang, Y., Li, Y., Tang, J., Wang, Z., Tang, J., Hu, K., 2017. Facile synthesis of tea waste/Fe_3O_4 nanoparticle composite for hexavalent chromium removal from aqueous solution. RSC Adv. 7, 7576–7590. https://doi.org/10.1039/C6RA27781K.

Garg, V.K., Kataria, N., 2016. Nanomaterial-based Sorbents for the Removal of Heavy Metal Ions from Water in Edited Book, Advanced Nanomaterials for Wastewater Remediation. CRC Press, Taylor & Francis Group, Boca Raton, Florida (USA), pp. 179–200.

Gautam, R.K., Sharma, S.K., Mahiya, S., Chattopadhyaya, M.C., 2014. Contamination of Heavy Metals in Aquatic Media: Transport, Toxicity and Technologies for Remediation, Heavy Metals in Water: Presence, Removal and Safety. Royal Society of Chemistry (RSC) Publishing, pp. 1–24.

Gupta, V.K., Ali, I., 2000. Utilisation of bagasse fly ash (a sugar industry waste) for the removal of copper and zinc from wastewater. Separ. Purif. Technol. 18, 131–140. https://doi.org/10.1016/S1383-5866(99)00058-1.

He, K., Chen, Y., Tang, Z., Hu, Y., 2016. Removal of heavy metal ions from aqueous solution by zeolite synthesized from fly ash. Environ. Sci. Pollut. Res. 23, 2778–2788. https://doi.org/10.1007/s11356-015-5422-6.

Iqbal, M., Saeed, A., Zafar, S.I., 2009. FTIR spectrophotometry, kinetics and adsorption isotherms modeling, ion exchange, and EDX analysis for understanding the mechanism of Cd^{2+} and Pb^{2+} removal by mango peel waste. J. Hazard Mater. 164, 161–171. https://doi.org/10.1016/j.jhazmat.2008.07.141.

Jain, M., Garg, V.K., Kadirvelu, K., 2013. Cadmium (II) sorption and desorption in a fixed bed column using sunflower waste carbon calcium–alginate beads. Bioresour. Technol. 129, 242–248. https://doi.org/10.1016/j.biortech.2012.11.036.

Joshi, S., Garg, V.K., Kataria, N., Kadirvelu, K., 2019. Applications of Fe_3O_4@AC nanoparticles for dye removal from simulated wastewater. Chemosphere 236, 124280. https://doi.org/10.1016/j.chemosphere.2019.07.011.

Joshi, S., Garg, V.K., Saini, J., Kadirvelu, K., 2018. Removal of Toulidine Blue O Dye from Aqueous Solution by Silica-Iron Oxide Nanoparticles. Mater. Focus. 7 (1), 140–146. https://doi.org/10.1166/mat.2018.1491.

Kataria, N., Garg, V.K., 2018a. Optimization of Pb (II) and Cd (II) adsorption onto ZnO nanoflowers using central composite design: isotherms and kinetics modelling. J. Mol. Liq. 271, 228–239. https://doi.org/10.1016/j.molliq.2018.08.135.

Kataria, N., Garg, V.K., 2018b. Green synthesis of Fe_3O_4 nanoparticles loaded sawdust carbon for cadmium (II) removal from water: regeneration and mechanism. Chemosphere 208, 818–828. https://doi.org/10.1016/j.chemosphere.2018.06.022.

Kataria, N., Garg, V.K., 2019. Application of EDTA modified Fe_3O_4/sawdust carbon nanocomposites to ameliorate methylene blue and brilliant green dye laden water. Environ. Res. 172, 43–54. https://doi.org/10.1016/j.envres.2019.02.002.

Langergren, S., Svenska, B.K., 1898. Zur theorie der Sogenanaken adsorption. Geloster Stoffe Veterns Apsakad Handle 24, 1–39.

Langmuir, I., 1916. The constitution and fundamental properties of solids and liquid. J. Am. Chem. Soc. 38, 2221–2295.

Langmuir, I., 1918. The adsorption of gases on plane surface of glass, mica and platinum. J. Am. Chem. Soc. 40, 136–140.

Liu, L., Fan, S., Li, Y., 2018. Removal behaviour of methylene blue from aqueous solution by tea waste: kinetics, isotherms and mechanism. Int. J. Environ. Res. Publ. Health 15, 1321. https://doi.org/10.3390/ijerph15071321.

Malkoc, E., Nuhoglu, Y., 2007. Potential of tea factory waste for chromium (VI) removal from aqueous solutions: thermodynamic and kinetic studies. Separ. Purif. Technol. 54, 291–298. https://doi.org/10.1016/j.seppur.2006.09.017.

Mckay, G., Ho, Y.S., 1999. Pseudo-second order model for sorption processes. Process Biochem. 34, 451–465. https://doi.org/10.1016/S0032-9592(98)00112-5.

Mohammed, R.R., 2012. Removal of heavy metals from waste water using black teawaste. Arab. J. Sci. and Eng. 37, 1505–1520. https://doi.org/10.1007/s13369-012-0264-8.

Otero, M., Rozada, F., Morán, A., Calvo, L.F., García, A.I., 2009. Removal of heavy metals from aqueous solution by sewage sludge based sorbents: competitive effects. Desalination 239, 46–57. https://doi.org/10.1016/j.desal.2008.03.005.

Pal, D., Maiti, S.K., 2019. Abatement of cadmium (Cd) contamination in sediment using tea waste biochar through meso-microcosm study. J. Clean. Prod. 212, 986–996. https://doi.org/10.1016/j.jclepro.2018.12.087.

Pirbazari, A.E., Pargami, N.R., Ashja, N., Emami, M.S., 2015. Surfactant-coated tea waste: preparation, characterization and its application for methylene blue adsorption from aqueous solution. J. Environ. Anal. Toxicol. 5, 1000310. https://doi.org/10.4172/2161-0525.1000310.

Saini, J., Garg, V.K., Gupta, R.K., 2018a. Green synthesized SiO_2@ OPW nanocomposites for enhanced Lead (II) removal from water. Arab .J .Chem. 13, 2496–2507. https://doi.org/10.1016/j.arabjc.2018.06.003.

Saini, J., Garg, V.K., Gupta, R.K., 2018b. Removal of Methylene Blue from aqueous solution by Fe_3O_4@Ag/SiO_2 nanospheres: synthesis, characterization and adsorption performance. J. Mol. Liq. 250, 413–422. https://doi.org/10.1016/j.molliq.2017.11.180.

Smith, J.M., Ness, H.C.V., 1987. Introduction to Chemical Engineering Thermodynamics. McGraw-Hill, New York, USA.

Temkin, M.J., Pyzhe, V., 1940. Recent modification to Langmuir isotherms. Acta Physiochim 12, 217–222.

Thakur, L.S., Parmar, M., 2013. Adsorption of heavy metal (Cu^{2+}, Ni^{2+} and Zn^{2+}) from synthetic wastewater by tea waste adsorbent. Int. J. Chem. Phys. Sci. 2, 6–19.

Wan, S., Ma, Z., Xue, Y., Ma, M., Xu, S., Qian, L., Zhang, Q., 2014. Sorption of lead (II), cadmium (II), and copper (II) ions from aqueous solutions using tea waste. Ind. Eng. Chem. Res. 53, 3629–3635. https://doi.org/10.1021/ie402510s.

Wen, T., Wang, J., Yu, S., Chen, Z., Hayat, T., Wang, X., 2017. Magnetic porous carbonaceous material produced from tea waste for efficient removal of as (V), Cr (VI), humic acid, and dyes. ACS Sustain. Chem. Eng. 5, 4371–4380. https://doi.org/10.1021/acssuschemeng.7b00418.

Weng, C.H., Lin, Y.T., Chen, Y.J., Sharma, Y.C., 2013. Spent green tea leaves for decolourisation of raw textile industry wastewater. Color. Technol. 129, 298–304. https://doi.org/10.1111/cote.12029.

Xiong, C., Wang, W., Tan, F., Luo, F., Chen, J., Qiao, X., 2015. Investigation on the efficiency and mechanism of Cd (II) and Pb (II) removal from aqueous solutions using MgO nanoparticles. J. Hazard Mater. 299, 664–674. https://doi.org/10.1016/j.jhazmat.2015.08.008.

Yang, X., Cui, X., 2013. Adsorption characteristics of Pb (II) on alkali treated tea residue. Water Resour. Ind. 3, 1–10. https://doi.org/10.1016/j.wri.2013.05.003.

Yu, S., Zhai, L., Wang, Y., Liu, X., Xu, L., Cheng, L., 2015. Synthesis of magnetic chrysotile nanotubes for adsorption of Pb (II), Cd (II) and Cr (III) ions from aqueous solution. J. Environ. Chem. Eng. 3, 752–762. https://doi.org/10.1016/j.jece.2015.03.023.

Zhu, Q., Li, Z., 2015. Hydrogel-supported nanosized hydrous manganese dioxide: synthesis, characterization, and adsorption behaviour study for $Pb^{2+,}$ $Cu^{2+,}$ Cd^{2+} and Ni^{2+} removal from water. Chem. Eng. J. 281, 69–80. https://doi.org/10.1016/j.cej.2015.06.068.